

# Mechanical Search on Shelves using Lateral Access X-RAY

Huang Huang<sup>\*1</sup>, Marcus Dominguez-Kuhne<sup>\*1,2</sup>, Jeffrey Ichnowski<sup>1</sup>, Vishal Satish<sup>1</sup>, Michael Danielczuk<sup>1</sup>, Kate Sanders<sup>1</sup>, Andrew Lee<sup>1</sup>, Anelia Angelova<sup>3</sup>, Vincent Vanhoucke<sup>3</sup>, Ken Goldberg<sup>1</sup>

**Abstract**—Efficiently finding an occluded object with lateral access arises in many contexts such as warehouses, retail, healthcare, shipping, and homes. We introduce LAX-RAY (Lateral Access maXimal Reduction of occupancY support Area), a system to automate the mechanical search for occluded objects on shelves. For such lateral access environments, LAX-RAY couples a perception pipeline predicting a target object occupancy support distribution with a mechanical search policy that sequentially selects occluding objects to push to the side to reveal the target as efficiently as possible. Within the context of extruded polygonal objects and a stationary target with a known aspect ratio, we explore three lateral access search policies: Uniform, Distribution Area Reduction (DAR) and Distribution Entropy Reduction over  $n$  Steps (DER- $n$ ) utilizing the support distribution and prior information. We evaluate these policies using the First-Order Shelf Simulator (FOSS) in which we simulate 800 random shelf environments of varying difficulty, and in a physical shelf environment with a Fetch robot and an embedded PrimeSense RGBD Camera. Average simulation results of 87.3% success rate demonstrate better performance of DER-2. Physical results show a success rate of at least 80% for DAR and DER- $n$ , suggesting that LAX-RAY can efficiently reveal the target object in reality. Both results show significantly better performance of DAR and DER- $n$  compared to the uniform policy with uniform probability distribution assumption in non-trivial cases, suggesting the importance of distribution prediction. Code, videos, and supplementary material can be found at <https://sites.google.com/berkeley.edu/lax-ray>.

## I. INTRODUCTION

While researchers have explored the problem of mechanical search in unstructured clutter (in which objects have significant freedom in both position and orientation) [5, 6], mechanical search in structured, lateral access environments such as shelves, cabinets, and closets is a less studied area despite its wide applicability. For instance, a service robot at a pharmacy or hospital may need to find supplies from a cabinet, an industrial robot may need to find kitting tools from shelves in warehouses, or a service robot in a retail store may need to search shelves for requested products from customers. Searching for an object in a lateral access environment poses new challenges not faced in unstructured environments, namely, limited action spaces, complex motion planning requirements, and a potentially limited perception view.

Research on grasping objects in structured clutter, including in lateral access environments is also present in the literature [9, 22, 24]. However, few papers focus on

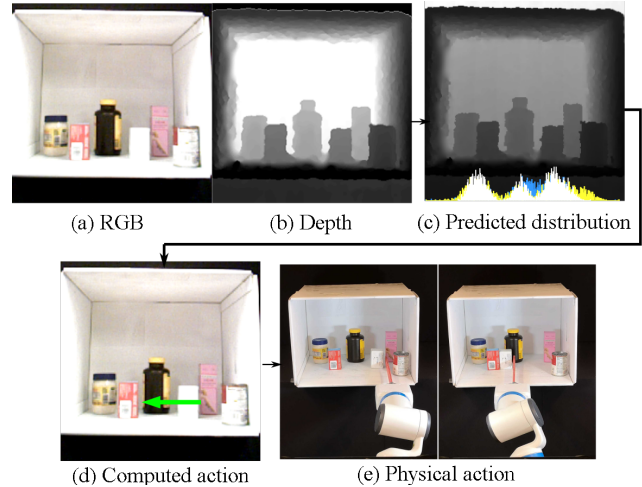


Fig. 1: **Lateral-access mechanical search with LAX-RAY.** The search starts with an RGB Image (a) and Depth Image (b) of the environment. LAX-RAY perception predicts a distribution (c) of where the search target is hidden: at the current step (yellow), the previous time step (blue), and the minimum of the two (white). The policy computes a push action (d) indicated by the green arrow, and (e) the robot executes it.

the problem of searching for occluded objects in lateral access environments as opposed to grasping visible ones. A natural approach for searching for an object in lateral access environments is to iteratively look behind objects that could be occluding the target object. This can be improved through using an occupancy distribution identifying where an occluded target object could be hidden [5] and a policy estimating which objects should be pushed out of the way or removed given prior information about explored zones could greatly speed up the searching process.

This paper focuses on finding an occluded target object in a lateral access environment and considers a lateral-access variant of the *Mechanical Search* problem [6]. In [6], the target object is in a bin and occluded from a top-down view by other objects. The lateral access environment introduces additional constraints including stable object poses due to gravity and limited operating space, where pushing operations can be more efficient. In this work, we extend X-RAY [5], a policy previously designed for bins with vertical access, to the lateral-access environment where all objects are resting in stable poses on a level shelf. We work within a shelf as opposed to the infinite planar workspace X-RAY assumes. We adapt the occupancy distribution prediction method in [5] to the lateral access environment and additionally utilize prior information. Instead of grasping to remove

<sup>\*</sup>These authors contributed equally. <sup>1</sup>The AUTOLab at University of California, Berkeley. <sup>2</sup>The California Institute of Technology. <sup>3</sup>Robotics at Google.

objects on an infinite plane, we consider stable translation pushing actions in a tightly constrained shelf.

This paper proposes LAX-RAY, a lateral access mechanical search system. Fig. 1 shows a diagram of LAX-RAY. Fig. 2 shows an example of a push planned by LAX-RAY. The contributions of this study are as follows:

- 1) An extension of the X-RAY deep-geometric inference system [5] to lateral-access environments predicting occupancy distribution.
- 2) Three lateral access mechanical search policies: Uniform, DAR and DER- $n$  ( $n \in \{1, 2, 3\}$ ) that compute actions to reveal occluded target objects stored on shelves.
- 3) The First Order Shelf Simulator (FOSS), a fast, open access, lightweight framework for generating initial shelf configurations and rapidly rolling out lateral search policies on them.
- 4) Experiments in simulation and on a physical robot validating the policies. Results from 800 simulated and 5 physical trials suggesting that DAR and DER-2 have better performance with less and more objects respectively.

## II. RELATED WORK

While we most notably take influence from work done in interactive perception and mechanical search [3, 6, 14, 19, 25, 30], work related to this problem spans back as far as the 1940s, such as Bayesian search: the problem of searching for one or more objects located in one of  $m$  locations [16]. Assaf *et al.* [1] illustrate that, in many cases, this problem has an optimal greedy solution. Their work is expanded on by Kress *et al.* [18], Lavis *et al.* [21], and Wen *et al.* [26], who consider cases of false-positive target detection, moving targets, and the production of sequences of optimal actions, respectively.

In robotics, LaValle *et al.* [20] consider the problem of moving a target object through clutter without obscuring it behind other objects and propose online algorithms that attempt to maximize object visibility in future time steps. Bitton *et al.* [2] illustrate methods for locating targets with multiple human and automated agents, and Novkovic *et al.* [23] introduce a reinforcement learning-based system for exploring unknown environments and searching for target objects. Yang *et al.* [28] approach the search problem by using a target-centric motion critic that is trained on observations and metadata mapped to rewards, and Murali *et al.* [22] use a collision checking model to grasp objects in the way until the target object is uncovered. In this study, we avoid potential collisions by estimating the depth difference between objects.

This task of searching for hidden objects is formalized and explored in the context of bin picking by Danielczuk *et al.* [6] and Kurenkov *et al.* [19]. In their papers on mechanical search they consider the problem of uncovering, identifying, and extracting a target object from clutter. Danielczuk *et al.* [6] explore a set of policies that select pushing actions either randomly or by prioritizing objects to push based

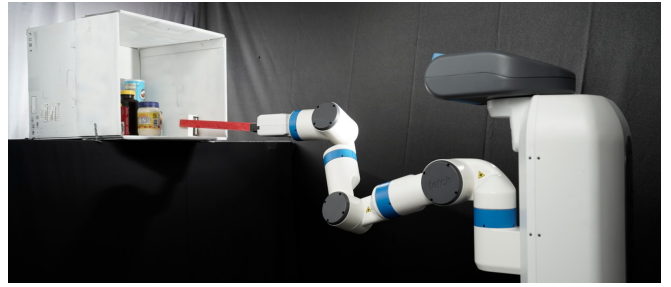


Fig. 2: The physical experiment with a Fetch robot and a shelf environment with random objects. The robot pushes an object a distance and direction calculated by LAX-RAY taking inputs of a RGBD image from the embedded PrimeSense camera .

on factors such as size. These policies were improved by the X-RAY system [5]—a neural network approach trained on thousands of simulated observations and target object occupancy distributions that predicts which areas of a scene are most likely to occlude the target object.

As we specifically consider the task of extracting a target object from a lateral environment, pushing is a critical action for moving objects out of the way. Significant developments have recently been made in the study of singulating cluttered objects on a plane [4, 7, 10, 11, 15, 17, 32]. Notably, Hermans *et al.* [15] propose a pushing policy that includes a history of past actions used to determine when termination should occur. Zeng *et al.* [31] consider the problem of grasping in clutter by implementing robotic pushing and grasping actions and develop synergies between them through deep reinforcement learning. Yang *et al.* [29] explore grasping in clutter through a pushing and grasping policy that makes use of a deep Q-learning network. This removes the need to generate training datasets as the training process for the policy is self-supervised. Eitel *et al.* [12] select push actions through the use of a neural network trained on physical data collected from robots interacting with cluttered scenes. The majority of the environments explored in these studies have relaxed constraints regarding object configurations and possible pushing actions compared to environments such as shelves, where a limited number of pushing actions are viable.

## III. PROBLEM STATEMENT

We consider an instance of the mechanical search problem in a lateral access environment (e.g., shelf). In this problem, an agent searches for the target object that is in a stable pose on a shelf, occluded behind other objects on the shelf. The target object has a known geometry, and the searching agent has RGBD camera with a fixed side-view of the shelf. The agent can push objects on the shelf to the left and right to search for the object, but cannot remove objects.

We have the following assumptions:

- Exactly one instance of the search target exists in the environment.
- All objects are extruded polygons without stacking.
- Toppling does not occur.
- The target object is not moved.



Fig. 3: Target objects used in simulation testing (left) and in physical experiments (right).

We represent the states of the system  $s(t) = \{Z_t, p_t, p'_{t-1}\}$ , where  $Z_t \in \mathbb{R}^{w \times h}$  is the current depth image,  $p_t(x, y)$  is the current 2D predicted target occupancy distribution, and  $p'_{t-1}(x, y)$  is the 2D history minimum predicted target occupancy probability computed at the previous time step. Both  $p_t(x, y)$  and  $p'_{t-1}(x, y)$  are outputs from a perception pipeline we will introduce in IV-A.

The robot takes actions  $a(t) = (D, d, (x, z))$ , where  $D \in \{L, R\}$  is the pushing direction (left or right), and  $d \in \mathbb{R}^+$  is the pushing distance. The coordinate  $(x, z)$  is the pushing starting point in the camera frame.

We define  $P(x, t)$ , a 1D occupancy distribution and the cost function  $c(t)$ , the negative cross entropy of the occupancy distribution as follows,

$$p'_t(x, y) = \min(p_t(x, y), p'_{t-1}(x, y)), \quad (1)$$

$$P(x, t) = \sum_{y=0}^{h-1} p'_t(x, y), \quad (2)$$

$$c(t) = - \sum_{i=0}^{w-1} P(x_i, t) \log(P(x_i, t)), \quad (3)$$

where  $h, w$  is the depth image height and width.

#### IV. METHODS

We propose LAX-RAY, an automated system combining (1) a perception pipeline to predict the target object occupancy distribution with (2) a search policy utilizing this information to solve the problem efficiently. The perception pipeline predicts an occupancy distribution for the (partially) occluded target object that spans across the visible objects in the scene given the depth image and target object segmentation mask. The search policy then computes the pushing action given a history of outputs from the perception module and the current observation at each step to efficiently uncover the target object.

##### A. LAX-RAY Perception

To predict an occupancy distribution for occluded and partially occluded objects from a depth image, we pre-train a neural network on synthetic data. This model predicts the target object's location in the image plane.

To generate large amounts of training data, we use a simulation (based on Trimesh [8]) with the constraints introduced by the lateral access environment. To generate data, the simulation first puts the target at a uniformly random position on a shelf. Occluding objects are then placed randomly on the shelf with no collisions. Due to the aspect ratio's dominating effect on the occupancy distribution we used five cuboid

target objects with varying aspect ratios (from 1:2 to 4:1 shown in Fig. 3) to train for varying target objects.

For each target object, we uniformly sampled transformations in the camera frame, with 14 translations in the  $x$  direction, 16 translations in the  $z$  direction, and 8 rotations in the  $x$ - $z$  plane. This gives us 1792 transformations per target object, which empirically works well.

After populating the simulated shelf environment, we render a  $256 \times 256$  depth image and the corresponding target segmentation mask using iGibson [27]. We use the latter in conjunction with the target segmentation mask for each possible transformation above to generate the ground truth occupancy distribution over all possible transformations as in [5]. To mitigate the uncertainty of the camera position in physical experiments, we render observations from 5 random (uniformly sampled) camera positions for each populated simulation environment.

We render over 30,000 images of training data for 5 target objects with occluding objects from the Google Scanned Objects dataset [13] in total. About 50% of these images include a fully occluded target object. We split the data into training and validation sets with a 4:1 ratio. We also render 10000 images from a separate group of object models with different target objects with similar aspect ratios as the test set as shown in Fig. 3. The occluding objects in the test set have different categories with different shapes.

We train a fully-connected network (FCN) with a ResNet backbone with 33 million parameters on the rendered data set using stochastic gradient descent with a momentum 0.99 for 60000 iterations with batch size 32 and learning rate  $10^{-5}$ . This network takes input of the target object segmentation mask as well as the depth image of the current shelf and outputs the occupancy distribution density map of the target object.

##### B. Search Policies

The search policy computes an action  $a(t) = (D, d, (x, z))$  defined above to take at each step to find the target object. A segmentation mask, generated based on significant depth discontinuities present in lateral access, is used to determine starting point candidates  $x$ . We restrict the pushing starting point  $y$  in camera frame to be a fixed relatively low height to avoid toppling.

The blade insertion depth  $z$  is directly proportional to the width of the object being pushed. The horizontal pushing distance  $d$  is the distance the object can be pushed until collision calculated by a highly negative depth gradient from  $Z_t$ , which is unique for each pair of  $(D, (x, z))$ . Thus, for each object, our policy aims to explore which object to push, implied by  $x$  and which direction  $D$  to push.

Using the occupancy distribution from the perception pipeline, we define the following search policies to locate the target object efficiently:

**Distribution Area Reduction (DAR)** ranks available actions using the current depth image and for every object computes the summed overlap of the object mask and the 1D minimum predicted occupancy distribution  $P(x, t)$ . The

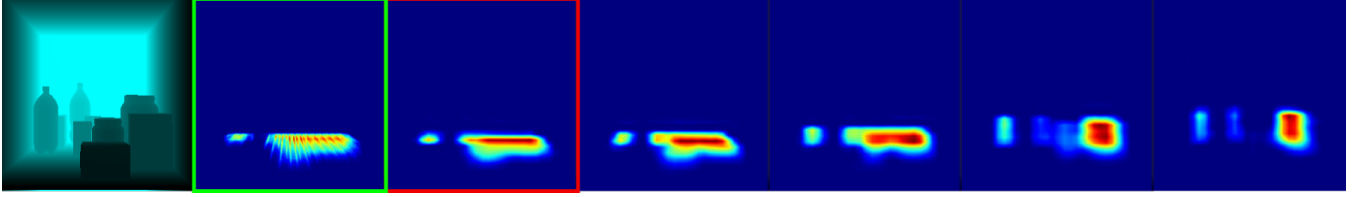


Fig. 4: Simulation validation results from test set for target object with 1:2 aspect ratio in a fully occluded case, where the left (first) image is the depth observation in simulation, the second image in **green** box is the ground truth occupancy distribution and the third image in **red** box is the prediction output corresponding to the correct target aspect ratio. The fourth to the last images shows the network prediction given aspect ratio from 1:1 to 4:1 respectively. Significant difference between the predictions implied the critical influence of target aspect ratios.

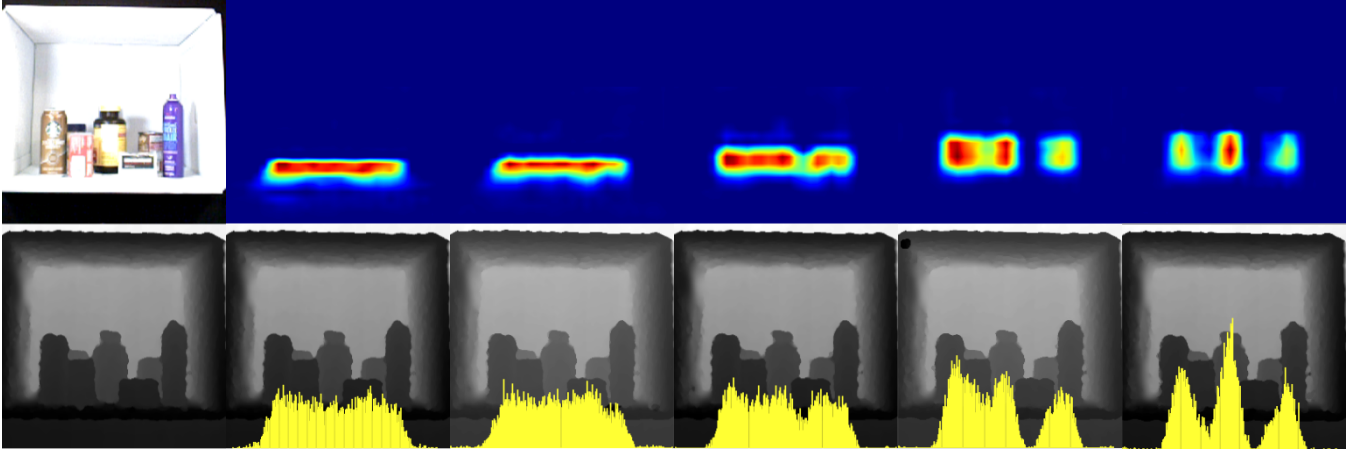


Fig. 5: Validation of the pre-trained model on physical experiment environment for 5 different target object with aspect ratios from 1:2 to 4:1 in a fully occluded case. The left column shows the color observation of the shelf with random objects and the corresponding depth image taken by the PrimeSense camera. The top row shows 2D occupancy distribution from the pre-trained model and the second row shows the corresponding 1D occupancy distribution along X axis in camera frame overlaid with the depth observation. A significant difference for predictions of each aspect ratio is shown validating the accuracy of the pre-trained model for real applications.

policy selects the action that reduces this sum the most. If the target object is partially revealed, the policy takes no action that would cover the target more.

**Distribution Entropy Reduction over  $n$  steps (DER- $n$ )** computes the 1D predicted distribution  $\hat{P}_{t+n}$  after taking  $n$  actions and chooses the action that it predicts to produce the smallest entropy value  $\hat{c}(t+n)$  at time step  $t+n$  if optimal actions are taken given the current information, where  $n \geq 1$ . It predicts  $\hat{P}_{t+n}$  by first predicting the depth image through translating the depth values of the object segmentation mask on the current depth image with the assumption of no other objects are behind. Then we get the occupancy distribution for this new depth image to get the predicted states.

**Uniform** is created by substituting the predicted occupancy distribution from DAR with a uniform distribution for places with occluding objects. It does not benefit from the perception pipeline.

## V. FIRST ORDER SHELF SIMULATOR (FOSS)

To validate the proposed policies, we propose a First Order Shelf Simulator (FOSS), a Python-based simulator that uses Trimesh [8] and Pyrender to model object-object interactions within a parametrizable shelf environment.

FOSS represents objects as extruded polygons (cuboids

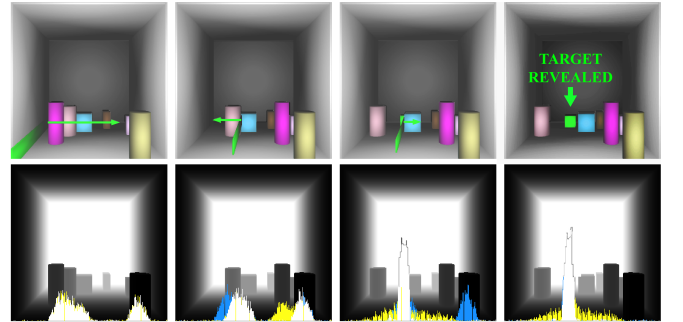


Fig. 6: The DER-1 policy reveals a hidden object with 6 occluding objects. First row shows color images at each step with a green blade, and a green arrow denoting push direction and distance. The occupancy distribution at the bottom of each depth image (second row) includes: predicted distribution from previous time step (**blue**), predicted distribution at current time step (**yellow**), and minimum of the two (**white**). Target is revealed in last image, where the occupancy distribution has a very dense probability.

and cylinder approximations) with pose constraints matching the problem statement. Cuboids uniformly range from 0.02 to 0.10 m for the square base and are 0.1 m tall. Cylinders uniformly range from 0.02 to 0.05 m for the base radius and are between 0.1 and 0.2 m tall, also sampled uniformly. A green target object cube with sides of size 0.07 m and aspect ratio of 1:1 is used. Action  $a(t)$  given by the policy

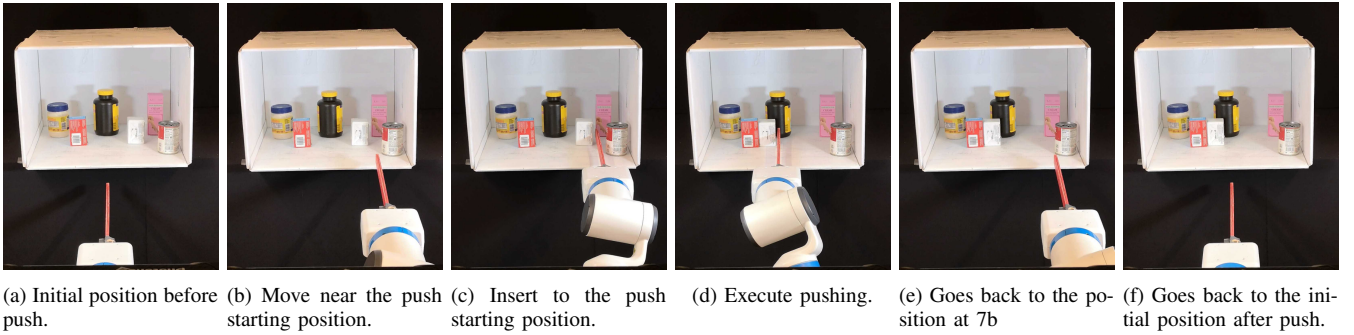


Fig. 7: 5 pushing steps for each pushing action.

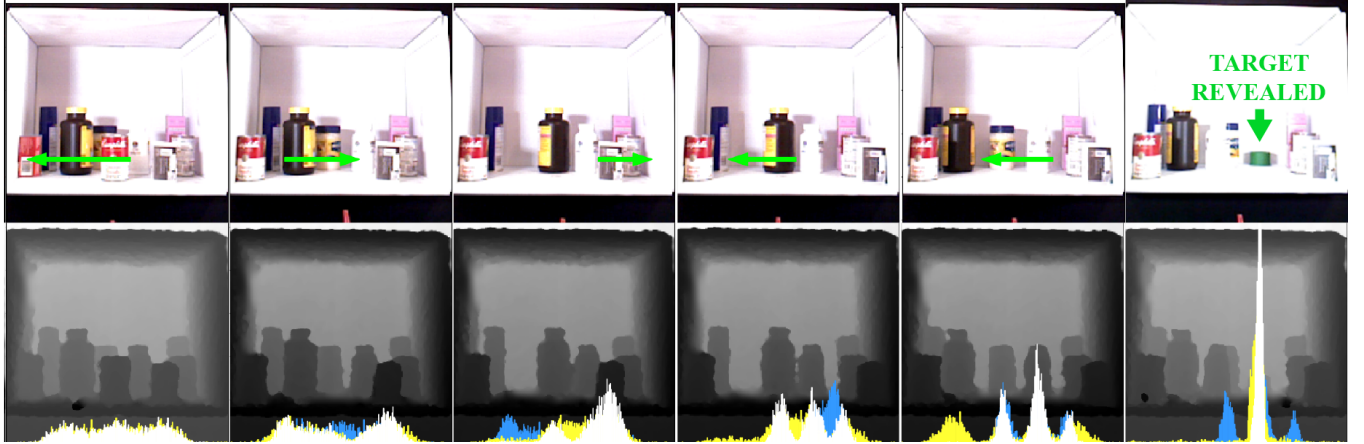


Fig. 8: The DER-1 policy reveals the target object among 9 occluding objects in a physical experiment. The plotted occupancy distributions at the bottom of each depth image including three parts: the predicted distribution from the previous time step (blue), the predicted distribution at the current time step (yellow), and minimum of the two distributions (white). **Left:** the target position and depth image. Each subsequent column shows the action output over time. **Top:** RGB image with green push action arrow denoting the pushing direction and distance. **Bottom:** depth image with occupancy distributions.

is executed without friction. FOSS checks collisions between targets and shelf wall. If an object collides with another object during the push, both objects move together for the remainder of the push in the push direction. When an object collides with the shelf wall, the push action stops.

Although FOSS allows for pushes in 2D, we focus on 1D lateral pushes in this paper. For simulation runs we place objects randomly on the shelf while checking for collisions to ensure object separation. Furthermore, to guarantee possible initial pushes, objects are initialized with at least the blade thickness away from the wall. Ground truth segmentation masks are used in FOSS.

## VI. EXPERIMENTS

We tested the perception system and the proposed policies both in simulation and physical environment.

### A. Perception Experiments in Simulation

In the simulation environment, images from both validation and test sets are used to benchmark the model, yielding a validation IoU of 0.79 and a test IoU of 0.53. Example images from the test set are shown in Fig. 4 in the case where the target object is fully occluded. The predicted distributions vary significantly across target object aspect ratios, indicating

that the distributions are particularly sensitive to the aspect ratio.

### B. Perception Experiments in Physical

In physical experiments, we use green target objects with similar sizes and aspect ratios to those used in simulation, including cuboids and cylinders, as shown in Fig. 3. We put random objects on a white shelf and use a PrimeSense RGBD camera embedded on a Fetch robot to get the color and depth images. We use a color detection algorithm on the color image by setting thresholds for RGB values to detect the target object, which is painted green. Fig. 5 shows the prediction results of the pre-trained model on a shelf with randomly arranged objects in a fully occluded case for all five target objects.

### C. Mechanical Search Policy Experiments in Simulation

We use FOSS to rapidly test our policies in many scenarios. For this, we use a randomly generated assortment of cylinders and boxes, such that their positions and sizes are random within the shelf and the range specified in Section V. All objects satisfy the pose constraints and are on the floor of the shelf in stable poses.

We generated 200 random scenes with 2, 4, 6, and 8 occluding objects respectively, giving us 800 scenes in total.

TABLE I: Simulation results for 5 policies over the same 200 simulation setups. For different number of occluding objects, the first row is the **Success Rate** followed by the **Average** of Steps and **Standard Deviation** of steps. As DER-n assume no unseen objects are behind the pushed object, DER-n policies have higher prediction errors as n increases. Addressing this is an important topic for future research.

No.	Results	Uniform	DAR	DER-1	DER-2	DER-3
2	Succ.	97%	<b>98%</b>	<b>98%</b>	97%	94%
	Step Avg	1.34	1.36	1.36	1.80	1.99
	Step Std	0.56	0.77	0.67	0.93	1.19
4	Succ.	88%	<b>96%</b>	92%	92%	89%
	Step Avg	2.27	2.33	2.37	2.57	3.21
	Step Std	1.48	1.78	1.79	1.93	2.02
6	Succ.	71%	87%	79%	<b>89%</b>	85%
	Step Avg	2.99	2.79	3.04	3.32	3.82
	Step Std	2.21	2.06	2.30	2.14	2.44
8	Succ.	46%	66%	63%	<b>71%</b>	66%
	Step Avg	3.61	3.40	3.13	3.94	4.08
	Step Std	2.75	2.47	2.25	2.65	2.54
Avg	Succ.	75.5%	86.8%	83.0%	<b>87.3%</b>	83.5%
	Step Avg	2.56	<b>2.47</b>	2.48	2.91	3.28

TABLE II: Physical experiment results. The first column shows the number of occluding objects. The remaining columns show **task success (top)** with Y denoting success and N denoting fail and the number of **actions to succeed (bottom number)**. The last row shows the average of the 5 experiments.

No.	Results	Uniform	DAR	DER-1	DER-2	DER-3
2	Success	Y	Y	Y	Y	Y
	Steps	3	3	3	1	1
4	Success	Y	Y	Y	Y	Y
	Steps	1	1	2	1	1
6	Success	Y	Y	Y	Y	Y
	Steps	3	4	4	6	6
7	Success	N	N	Y	Y	Y
	Steps	4	7	3	4	3
9	Success	N	Y	Y	Y	Y
	Steps	9	5	5	3	5
Avg	Success	60%	80%	<b>100%</b>	<b>100%</b>	<b>100%</b>
	Steps	4	4	3.4	<b>3</b>	3.2

We tested 3 prediction steps of DER-n for  $n \in \{1, 2, 3\}$  together with Uniform and DAR on each scene. A green cube with a 1:1 aspect ratio is used for the target. A rollout is considered successful if at least 90% of the target object is revealed within 10 actions. The policies' performance in simulation is summarized in Table I with a successful DER-1 policy rollout in Fig. 6.

Table I suggests DAR and the DER-n policies perform better than the Uniform policy, especially as the number of objects increases. This shows the contribution of the occupancy distribution. All policies' performances drop when the number of occluding objects increases since more steps are needed to reveal the target. DAR performs best when there are fewer than 6 occluding objects and DER-2 perform best in 6 or more objects scenarios. The prediction of the next step assumes no unseen objects are behind the pushed object, which can deviate from what actually happens. Thus, there is a tradeoff between the prediction errors and lookahead. Compared to DER-2, DER-1 performs worse because not enough future information is revealed while DER-3 performs worse because prediction error accumulates. When there are fewer objects, prediction errors dominate this tradeoff, which

could explain the better performance of DAR compared with DER-2.

Most failure cases for DAR and DER-1 occur due to not looking ahead. Without lookahead, DAR and DER-1 struggle in cases where multiple layers of objects block the target; they often will avoid pushing the front object since it does not immediately change the predicted distribution. DER-2 and DER-3 mitigate this issue by considering the total reward of pushing both layers of objects.

#### D. Mechanical Search Policy Experiments in Physical

To test the policies, we set up a shelf environment with random objects and execute the insertion and pushing actions using a Fetch robot with a blade attached to the gripper. An embedded PrimeSense camera is used for taking RGBD observations. Fig. 2 shows the setup. At each time step, we execute the pushing action returned by the policy in 5 steps starting and ending at the same fixed position as shown in Fig. 7. By dividing the pushing action into those 5 steps, we avoid the occlusion of the robot arm to the camera and any potential collisions.

We tested 5 different layouts for each policy with 2 occluding objects, 4 occluding objects, 6 occluding objects, 7 occluding objects and 9 occluding objects respectively. A target object with aspect ratio of 1:2 from Fig. 3 is used and is fully occluded in all layouts.

The performance of each policy is summarized in Table II. The results suggest consistency with the simulation results in which the uniform policy has the worst performance with the lowest success rate, and DER-2 shows the best performance with lowest average number of steps. Fig. 8 shows an action series for experiment 5 with DER-1.

## VII. CONCLUSION AND FUTURE WORK

This paper addresses the "lateral access" (shelf) variant of mechanical search and proposes three novel policies utilizing the additional constraints and the predicted target object occupancy distribution to optimize the number of pushing actions needed to reveal a target object on a shelf.

In future work, we will investigate more sophisticated depth models and the use of pushes parallel to the camera (depth) axis to create space for lateral pushes, and pull actions using pneumatically-activated suction cups to lift and remove occluding objects from the shelf.

## ACKNOWLEDGEMENTS

This research was performed at the AUTOLAB at UC Berkeley in affiliation with the Berkeley AI Research (BAIR) Lab. This research was supported in part by: NSF National Robotics Initiative Award 1734633 and by a Focused Research Award from Google Cloud. The authors were supported in part by donations from Google and Toyota Research Institute, the National Science Foundation Graduate Research Fellowship Program under Grant No. 1752814, and by equipment grants from PhotoNeo and NVidia. We thank our colleagues who provided helpful feedback and suggestions.

## REFERENCES

- [1] D. Assaf and S. Zamir, "Optimal sequential search: A bayesian approach," *The Annals of Statistics*, pp. 1213–1221, 1985.
- [2] E. Bitton and K. Goldberg, "Hydra: A framework and algorithms for mixed-initiative uav-assisted search and rescue," in *2008 IEEE International Conference on Automation Science and Engineering*, IEEE, 2008, pp. 61–66.
- [3] J. Bohg, K. Hausman, B. Sankaran, O. Brock, D. Kragic, S. Schaal, and G. S. Sukhatme, "Interactive perception: Leveraging action in perception and perception in action," *IEEE Transactions on Robotics*, vol. 33, no. 6, pp. 1273–1291, 2017.
- [4] L. Chang, J. R. Smith, and D. Fox, "Interactive singulation of objects from a pile," in *2012 IEEE International Conference on Robotics and Automation*, IEEE, 2012, pp. 3875–3882.
- [5] M. Danielczuk, A. Angelova, V. Vanhoucke, and K. Goldberg, "X-ray: Mechanical search for an occluded object by minimizing support of learned occupancy distributions," *arXiv preprint arXiv:2004.09039*, 2020.
- [6] M. Danielczuk, A. Kurenkov, A. Balakrishna, M. Matl, D. Wang, R. Martin-Martin, A. Garg, S. Savarese, and K. Goldberg, "Mechanical search: Multi-step retrieval of a target object occluded by clutter," in *2019 International Conference on Robotics and Automation (ICRA)*, IEEE, 2019, pp. 1614–1621.
- [7] M. Danielczuk, J. Mahler, C. Correa, and K. Goldberg, "Linear push policies to increase grasp access for robot bin picking," in *2018 IEEE 14th International Conference on Automation Science and Engineering (CASE)*, IEEE, 2018, pp. 1249–1256.
- [8] Dawson-Haggerty et al., *Trimesh*, version 3.2.0, Dec. 8, 2019.
- [9] M. Dogar, K. Hsiao, M. Ciocarlie, and S. Srinivasa, "Physics-based grasp planning through clutter," 2012.
- [10] M. Dogar and S. Srinivasa, "A framework for push-grasping in clutter," *Robotics: Science and systems VII*, vol. 1, 2011.
- [11] Z. Dong, S. Krishnan, S. Dolasia, A. Balakrishna, M. Danielczuk, and K. Goldberg, "Automating planar object singulation by linear pushing with single-point and multi-point contacts," in *2019 IEEE 15th International Conference on Automation Science and Engineering (CASE)*, IEEE, 2019, pp. 1429–1436.
- [12] A. Eitel, N. Hauff, and W. Burgard, "Learning to singulate objects using a push proposal network," in *Robotics Research*, Springer, 2020, pp. 405–419.
- [13] *Google scanned objects dataset*, <https://app.ignitionrobotics.org/GoogleResearch/fuel/collections/Google%20Scanned%20Objects>.
- [14] M. Gupta and G. S. Sukhatme, "Using manipulation primitives for brick sorting in clutter," in *2012 IEEE International Conference on Robotics and Automation*, IEEE, 2012, pp. 3883–3889.
- [15] T. Hermans, J. M. Rehg, and A. Bobick, "Guided pushing for object singulation," in *2012 IEEE/RSJ International Conference on Intelligent Robots and Systems*, IEEE, 2012, pp. 4783–4790.
- [16] B. O. Koopman, "Search and screening, operations evaluation group report 56," *Center for Naval Analysis, Alexandria, Virginia*, 1946.
- [17] M. Kopicki, J. Wyatt, and R. Stolkin, "Prediction learning in robotic pushing manipulation," in *2009 International Conference on Advanced Robotics*, IEEE, 2009, pp. 1–6.
- [18] M. Kress, K. Y. Lin, and R. Szechtman, "Optimal discrete search with imperfect specificity," *Mathematical methods of operations research*, vol. 68, no. 3, pp. 539–549, 2008.
- [19] A. Kurenkov, J. Taglic, R. Kulkarni, M. Dominguez-Kuhne, R. Martín-Martín, A. Garg, and S. Savarese, "Visuomotor mechanical search: Learning to retrieve target objects in clutter," in *IEEE/RSJ Int. Conference. on Intelligent Robots and Systems (IROS)*, 2020.
- [20] S. M. LaValle, H. H. González-Banos, C. Becker, and J.-C. Latombe, "Motion strategies for maintaining visibility of a moving target," in *Proceedings of International Conference on Robotics and Automation*, IEEE, vol. 1, 1997, pp. 731–736.
- [21] B. Lavis, T. Furukawa, and H. F. D. Whyte, "Dynamic space re-configuration for bayesian search and tracking with moving targets," *Autonomous Robots*, vol. 24, no. 4, pp. 387–399, 2008.
- [22] A. Murali, A. Mousavian, C. Eppner, C. Paxton, and D. Fox, "6-dof grasping for target-driven object manipulation in clutter," in *2020 IEEE International Conference on Robotics and Automation (ICRA)*, IEEE, 2020, pp. 6232–6238.
- [23] T. Novkovic, R. Pautrat, F. Furrer, M. Breyer, R. Siegwart, and J. Nieto, "Object finding in cluttered scenes using interactive perception," in *2020 IEEE International Conference on Robotics and Automation (ICRA)*, IEEE, 2020, pp. 8338–8344.
- [24] A. Saxena, L. Wong, M. Quigley, and A. Y. Ng, "A vision-based system for grasping novel objects in cluttered environments," in *Robotics research*, Springer, 2010, pp. 337–348.
- [25] H. Van Hoof, O. Kroemer, and J. Peters, "Probabilistic segmentation and targeted exploration of objects in cluttered environments," *IEEE Transactions on Robotics*, vol. 30, no. 5, pp. 1198–1209, 2014.
- [26] Z. Wen, B. Kveton, B. Eriksson, and S. Bhamidipati, "Sequential bayesian search," in *International Conference on Machine Learning*, 2013, pp. 226–234.
- [27] F. Xia, W. B. Shen, C. Li, P. Kasimbeg, M. E. Tchammi, A. Toshev, R. Marti'n-Marti'n, and S. Savarese, "Interactive gibson benchmark: A benchmark for interactive navigation in cluttered environments," *IEEE Robotics and Automation Letters*, vol. 5, no. 2, pp. 713–720, 2020.
- [28] Y. Yang, H. Liang, and C. Choi, "A deep learning approach to grasping the invisible," *IEEE Robotics and Automation Letters*, vol. 5, no. 2, pp. 2232–2239, 2020.
- [29] Z. Yang and H. Shang, "Robotic pushing and grasping knowledge learning via attention deep q-learning network," in *International Conference on Knowledge Science, Engineering and Management*, Springer, 2020, pp. 223–234.
- [30] A. Zeng, P. Florence, J. Tompson, S. Welker, J. Chien, M. Attarian, T. Armstrong, I. Krasin, D. Duong, V. Sindhwani, and J. Lee, *Transporter networks: Rearranging the visual world for robotic manipulation*, 2020. arXiv: 2010.14406 [cs.RO].
- [31] A. Zeng, S. Song, S. Welker, J. Lee, A. Rodriguez, and T. Funkhouser, "Learning synergies between pushing and grasping with self-supervised deep reinforcement learning," in *2018 IEEE/RSJ International Conference on Intelligent Robots and Systems (IROS)*, IEEE, 2018, pp. 4238–4245.
- [32] C. Zito, R. Stolkin, M. Kopicki, and J. L. Wyatt, "Two-level rrt planning for robotic push manipulation," in *2012 IEEE/RSJ international conference on intelligent robots and systems*, IEEE, 2012, pp. 678–685.